SPACE MAPPING OPTIMIZATION OF WAVEGUIDE FILTERS USING FINITE ELEMENT AND MODE-MATCHING ELECTROMAGNETIC SIMULATORS

J.W. Bandler, R.M. Biernacki,
S.H. Chen and D. Omeragić

OSA-96-MT-23-R

November 30, 1996

SPACE MAPPING OPTIMIZATION OF WAVEGUIDE FILTERS USING FINITE ELEMENT AND MODE-MATCHING ELECTROMAGNETIC SIMULATORS

J.W. Bandler, R.M. Biernacki, S.H. Chen and D. Omeragić*

Optimization Systems Associates Inc.
P.O. Box 8083, Dundas, Ontario
Canada L9H 5E7

Email osa@osacad.com URL http://www.osacad.com

Abstract

For the first time, we apply aggressive space mapping to automatically aligning electromagnetic models based on hybrid mode-matching/network theory simulations with models based on finite-element (FEM) simulations in the design optimization of microwave circuits. Statistical parameter extraction involving ℓ_1 and penalty concepts facilitates a key requirement by space mapping for uniqueness and consistency. EM optimization of an H-plane resonator filter with rounded corners illustrates the advantages as well as the challenges of our approach. The effects of manufacturing tolerances are rapidly estimated for the first time with FEM accuracy.

This work was supported in part by the Simulation Optimization Systems Research Laboratory and Department of Electrical and Computer Engineering, McMaster University, and in part by the Natural Sciences and Engineering Research Council of Canada under Grants OGP0007239, OGP0042444 and STR0167080 and through the Micronet Network of Centres of Excellence.

* D. Omeragić is with the Simulation Optimization Systems Research Laboeratory and Department of Electrical and Computer Engineering, mcMaster University, Hamilton, Ontario, Canada L8S 4L7.

Manuscript submitted December 2, 1996.

SUMMARY

Introduction

Direct exploitation of electromagnetic (EM) simulators in the optimization of arbitrarily shaped 3D structures at high frequencies is crucial for first-pass success CAD. Recently, we reported successful automated design optimization of 3D structures using FEM simulations [1].

In this paper, we apply for the first time, aggressive space mapping optimization [1,2] through automatic alignment of the results of two separate EM simulation systems. The objective of space mapping is to avoid direct optimization of computationally intensive models. The so-called optimization space (OS) in the present case is represented by a library of waveguide models based on mode matching (MM) connected by network theory: we use the RWGMM program developed by Arndt and his colleagues [3,4]. For the so-called EM space (EM) or "fine" model we have selected Maxwell Eminence [5].

Both simulation approaches provide accurate EM analysis. RWGMM is computationally efficient in its treatment of a variety of predefined geometries. It is ideally suited for modeling complex waveguide structures that can be decomposed into the available library building blocks. FEM-based simulators such as Maxwell Eminence [5] are able to analyze arbitrary shapes, but they are computationally very intensive.

We demonstrate aggressive space mapping optimization of an H-plane resonator filter with rounded corners. Subsequent Monte Carlo analysis of manufacturing tolerances exploits the FEM-based space mapped model with the speed of the MM/network theory simulator. We also successfully optimized waveguide transformers using space mapping that aligns hybrid MM/network theory simulations with a few modes (coarse model) and hybrid MM/network theory simulations using many modes to represent the discontinuities (fine model).

Particularly challenging in the present work is the parameter extraction phase, key to effective implementation of space mapping optimization. The space mapping methodology has been shown to be sensitive to nonunique solutions or local minima inconsistent with the design optimization solution we are aiming at. In this paper we present an in-depth study of this phenomenon and how it may be addressed. We offer a solution based on statistical parameter extraction involving a powerful ℓ_1 algorithm and penalty function concepts. We show that we can satisfy the requirement for uniqueness and consistency.

The software systems used to produce the results presented in this paper include the RWGMM library [3] linked with the network theory optimizers of OSA90/hope [6]. Maxwell Eminence was interfaced through Empipe3D [6]. The space mapping procedure executes all these systems concurrently.

Space Mapping Optimization Using MM/Network Theory and FEM

The space mapping optimization using the MM waveguide library serves as the OS model and the FEM simulator as the EM model. The flow diagram of our space mapping procedure is outlined in Fig. 1. We address the design of the H-plane resonator filter shown in Fig. 2. The waveguide cross-section is 15.8 × 7.9 mm, while the thickness of the irises is t = 0.4 mm. The radius of the corners is R = 1 mm. The iris and resonator dimensions d_1, d_2, l_1, l_2 are selected as the optimization variables.

First, minimax optimization of the OS model (Fig. 2(a)) is performed exploring the waveguide MM library with the following specifications provided by Arndt [7]

$$|S_{21}| \text{ (dB)} < -35 \quad \text{for } 13.5 \leq f \leq 13.6 \text{ GHz}$$

$$|S_{11}| \text{ (dB)} < -20 \quad \text{for } 14.0 \leq f \leq 14.2 \text{ GHz}$$

$$|S_{21}| \text{ (dB)} < -35 \quad \text{for } 14.6 \leq f \leq 14.8 \text{ GHz}$$

where f represents the frequency.

The minimax solution x_{os}^*, which yields the target response for space mapping, is d_1 = 6.04541, d_2 = 3.21811, l_1 = 13.06880, l_2 = 13.8841. The responses of the two models at this point are shown in Fig. 3.

Focusing on the passband, we treat responses in the region 13.96 ≤ f ≤ 14.24 GHz. The responses of both models at the point x_{os}^* are shown in Fig. 4. Fifteen sample points were used with Maxwell Eminence. Tables I, II and III summarize the steps of the successful space mapping optimization using the statistical parameter extraction procedure outlined in the next section. The optimized response shown in Fig. 5 was obtained after only 4 simulations by Maxwell Eminence.

We verified the space mapping results by directly optimizing the H-plane filter using Empipe3D [6] driving the FEM solver Maxwell Eminence [5]. The direct optimization results confirmed that our space mapping solution is indeed optimal.

Statistical Parameter Extraction

Space mapping has been shown to be sensitive to nonunique solutions [1] or local minima which are inconsistent with the design optimization solution we are aiming at. Here, we propose an automated statistical parameter extraction procedure to overcome potential pitfalls arising out of inaccurate or nonunique solutions.

First, we perform standard ℓ_1 parameter extraction [8] starting from $\boldsymbol{x}_{os}^*$. If the optimized response matches well the EM model response (the ℓ_1 objective is small enough) we continue with the space mapping iterations. Otherwise we turn to statistical exploration of the OS model.

The key to statistical parameter extraction is to establish the exploration region. Unlike a general purpose random/global optimization approach we want to carry out local statistical exploration as deemed suitable for space mapping. To this end we need to realize that in the process of space mapping the desired parameter extraction solutions, that is the points in the OS space, gradually approach $\boldsymbol{x}_{os}^*$ (see [2]). Furthermore, we may consider the concept of the consistency of the parameter extraction process w.r.t. the *existing* mapping.

Consider the kth space mapping step. When the existing mapping ($\boldsymbol{x}_{os} = \boldsymbol{P}^{(k-1)}(\boldsymbol{x}_{em})$) is applied to the current point in the EM model space we arrive at $\boldsymbol{x}_{os}^*$, since that point has been determined by the inverse mapping ($\boldsymbol{x}_{em}^k = \boldsymbol{P}^{(k-1)^{-1}}(\boldsymbol{x}_{os}^*)$, see [2]). The fact that the new point (to be extracted) will be different from $\boldsymbol{x}_{os}^*$ is not only the basis for modifying the mapping, but also quantitatively establishes the degree of inconsistency w.r.t. the existing mapping. This allows us to define an appropriate exploration region. For example, for the kth step, if we define the multidimensional interval $\boldsymbol{\delta}$ as

$$\boldsymbol{\delta} = \boldsymbol{x}_{os}^{k-1} - \boldsymbol{x}_{os}^* \qquad (2)$$

the statistical exploration may be limited to the region defined by

$$x_i = [\ x_{osi}^{\ *} - 2\ |\ \delta_i\ |,\ x_{osi}^{\ *} + 2\ |\ \delta_i\ |\ ] \tag{3}$$

A set of N_s starting points is then statistically generated within the region (3) and N_s parameter extraction optimizations are carried out. These parameter extractions are further aided by a penalty function [9] of the form

$$\lambda \, \| \, x_{os}^{\ k} - x_{os}^{\ *} \, \| \tag{4}$$

augmenting the ℓ_1 objective function. The resulting solutions (expected to be multiple) are then categorized into clusters and ranked according to the achieved values of the objective function. Finally, the penalty term is removed and the process repeated in order to focus the clustered solution(s). The aforementioned steps are briefly summarized by the following algorithm and illustrated in the flow chart shown in Fig. 6.

Algorithm

Step 1 Initialize the exploration region. If this is the first space mapping iteration this initialization is arbitrary; otherwise use (3).

Step 2 Generate N_s starting points.

Step 3 Perform N_s parameter extractions from the N_s starting points including the penalty function (4).

Step 4 Categorize the solutions. Select one or more best clusters of the solutions.

Step 5 Focus the clusters by reoptimizing without the penalty term.

This approach has been automated using a three-level Datapipe architecture, similar to [1]. Furthermore, it can be parallelized since the N_s parameter extractions considered are carried out independently.

Parameter Extraction of the H-Plane Filter

Fig. 7 presents the variation of the MM/network theory model response in the vicinity of the starting point. Responses are computed along the direction of the first aggressive space mapping step, defined by points $x_{os}^{\ *}$ and $x_{os}^{\ 1}$. Fig. 8 shows the variation of the ℓ_1 objective in the vicinity of the starting point w.r.t. two sensitive parameters: the iris openings d_1 and d_2. Obviously, the ℓ_1 objective function has multiple minima, hence the optimizer may terminate at an undesirable solution.

We apply the statistical extraction procedure outlined in the preceding section. A set of 100 starting points is statistically generated, using a uniform random number generator, within the range (3). The ℓ_1 parameter extraction optimization with the penalty term (4) is performed from these points. The distances of the random starting points and corresponding solutions from the point x_{os}^* are depicted in Fig. 9. The solutions are scattered, confirming our observation that the ℓ_1 objective function has many local minima as illustrated in Fig. 8. Among the 100 solutions a cluster of 15 points is detected in Fig. 9(b). Removing the penalty term and restarting the parameter extraction process from all the points further sharpens the solution, as shown in Fig. 9(b). All the points within the cluster converge to the same solution, as depicted in Fig. 9(c). Figs. 10 and 11 show the responses of the 100 points before and after the parameter extraction, respectively. Fig. 12 displays the responses corresponding to the cluster of 15 points which converged to the same solution, validating successful parameter extraction.

Space Mapping Optimization Using Coarse MM Model and Fine MM Model

The RWGMM library allows a designer to take into a large number of higher-order modes to model waveguide transition components. Increasing the number of modes improves accuracy at the expense of higher computational cost. Space mapping may enhance the efficiency of the MM-based optimization by aligning the response of the fine model (including many modes) with the response of a coarse model (using one or a few modes).

We apply this strategy to the optimization of three-section and seven-section transformers described in [10]. For the coarse model, we used just one mode. For the fine model, we included all the modes below the cut-off frequency. The actual number of modes included in the fine model is automatically determined by the RWGMM program. As the lengths and heights of the waveguide sections are optimized, the number of modes included in the fine model varies from 49 to 198. The space mapping optimization reached a solution in 4 steps.

Tolerance Simulation Using Space Mapping

Space mapping provides not only the optimized parameter values, but also an efficient means of statistical tolerance analysis. We can map parameter tolerances in the EM space to the corresponding incremental changes in the OS space. Consequently, we will be able to rapidly estimate the effects of manufacturing tolerances, benefitting at the same time from the accuracy of the FEM model and the speed of the hybrid MM/network theory simulations.

As an illustration, we consider Monte Carlo analysis of the H-plane filter. We assign normally distributed tolerances to all parameter values, with a standard deviation of 0.0333% (in the order of 1 μm). The Monte Carlo simulation results are shown in Fig. 13. Assuming a specification of $|S_{11}|$ (dB) < -15 in the passband, the estimated yield is 88.5% out of 200 outcomes. Then, we increased the standard deviations of the parameter tolerances to 0.1%. This time the yield dropped to 19% out of 200 outcomes.

By using the space mapping model, the CPU time required for the Monte Carlo analysis is comparable to just a single full FEM simulation.

Conclusions

We have presented new applications of aggressive space mapping to filter optimization using network theory, mode-matching and finite element simulation techniques. A statistical approach to parameter extraction incorporating the ℓ_1 objective and penalty function concepts has effectively addressed the requirement of a unique and consistent solution. We have also demonstrated space mapping optimization based on coarse and fine MM models with different numbers of modes. We have shown that the space mapping model provides a highly efficient means for rapid Monte Carlo analysis of microwave circuits with the accuracy of FEM simulation.

References

[1] J.W. Bandler, R.M. Biernacki and S.H. Chen, "Fully automated space mapping optimization of 3D structures," *IEEE MTT-S Int. Microwave Symp. Dig.*, (San Francisco, CA), 1996, pp. 753-756.

[2] J.W. Bandler, R.M. Biernacki, S.H. Chen, R.H. Hemmers and K. Madsen, "Electromagnetic optimization exploiting aggressive space mapping," *IEEE Trans. Microwave Theory Tech.*, vol. 43, 1995, pp. 2874-2882.

[3] T. Sieverding, U. Papziner, T. Wolf and F. Arndt, "New mode-matching building blocks for common circuit CAD programs," *Microwave Journal*, vol. 36, July 1993, pp. 66-79.

[4] F. Arndt, T. Sieverding, T. Wolf and U. Papziner, "Optimization-oriented design of rectangular and circular waveguide components using efficient mode-matching simulators in commercial circuit CAD tools," *Int. J. Microwave and Millimeter-Wave Computer-Aided Engineering*, vol. 7, 1997, (in press).

[5] *Maxwell Eminence*, Ansoft Corporation, Four Station Square, Suite 660, Pittsburgh, PA 15219.

[6] *OSA90/hope*™ and *Empipe3D*™, Optimization Systems Associates Inc., P.O. Box 8083, Dundas, Ontario, Canada L9H 5E7, 1996.

[7] F. Arndt, *Private communications*, Microwave Department, University of Bremen, P.O. Box 330 440, Kufsteiner Str., NW1, D-28334 Bremen, Germany, 1996.

[8] J.W. Bandler, S.H. Chen and S. Daijavad, "Microwave device modeling using efficient ℓ_1 optimization: a novel approach," *IEEE Trans. Microwave Theory Tech.*, vol. MTT-34, 1986, pp. 1282-1293.

[9] J.W. Bandler, R.M. Biernacki, S.H. Chen and Y.F. Huang, "Design optimization of interdigital filters using aggressive space mapping and decomposition," *IEEE Trans. Microwave Theory Tech.*, vol. MTT-45, 1997, (in press).

[10] J.W. Bandler, "Computer optimization of inhomogeneous waveguide transformers," *IEEE Trans. Microwave Theory Tech.*, vol. MTT-17, 1969, pp. 563-571.

TABLE I

SPACE MAPPING OPTIMIZATION OF THE H-PLANE FILTER

Point	d_1	d_2	l_1	l_2
x_{em}^1	6.04541	3.21811	13.06880	13.8841
x_{em}^2	6.19267	3.32269	12.98759	13.87521
x_{em}^3	6.17017	3.29692	13.05362	13.88117
x_{em}^4	6.17557	3.29058	13.02820	13.88411

Values of all optimization variables are in mm.

TABLE II

PARAMETER EXTRACTION RESULTS FOR SPACE MAPPING OPTIMIZATION

Point	d_1	d_2	l_1	l_2
x_{os}^1	5.89815	3.11353	13.1500	13.8930
x_{os}^2	6.07714	3.25445	12.9757	13.8757
x_{os}^3	6.03531	3.22421	13.1119	13.8806
x_{os}^4	6.04634	3.22042	13.0618	13.8831

Values of all optimization variables are in mm.

TABLE III

PARAMETER EXTRACTION - DISTANCES FROM x_{os}^*

Step	$\| x_{os}^* - x_{os}^i \|$
1	0.198234
2	0.105192
3	0.044823
4	0.007497

Values are in mm.

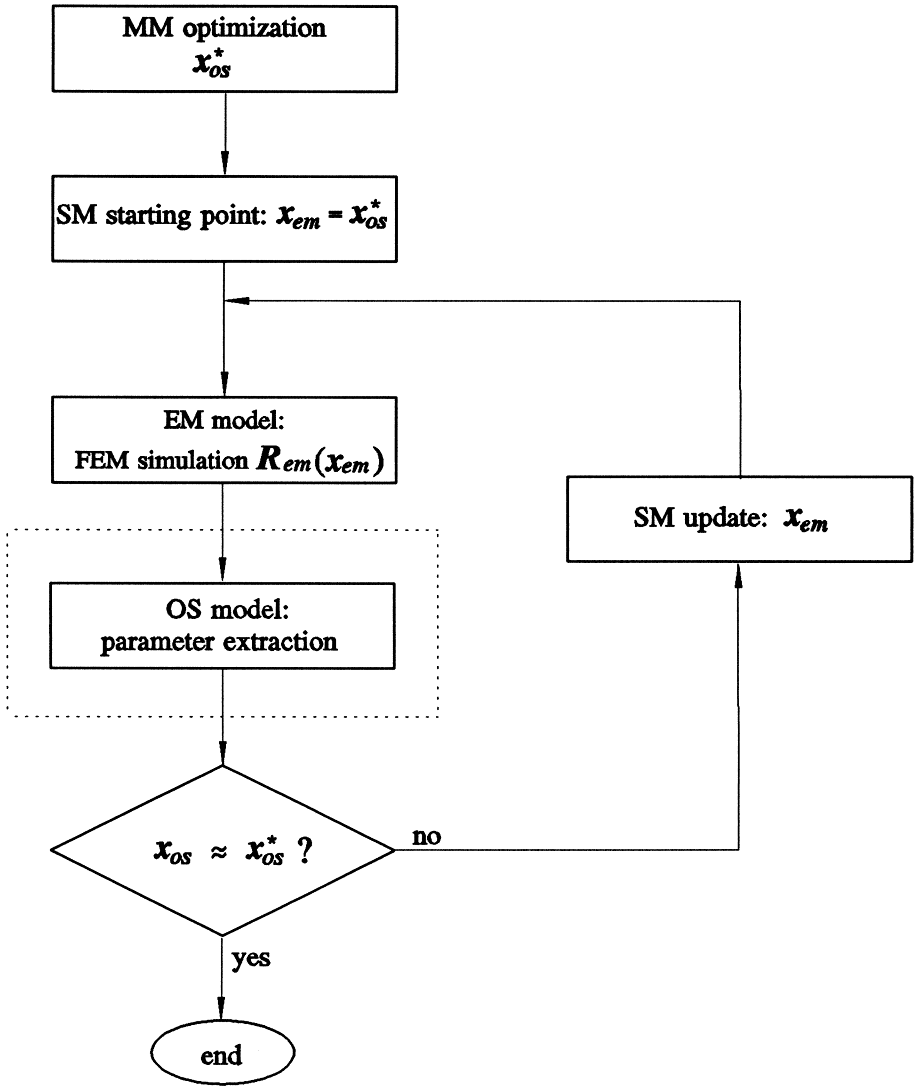

Fig. 1. Flow diagram of the space mapping optimization (SM) procedure concurrently exploiting the hybrid MM/network theory and FEM techniques and statistical parameter extraction.

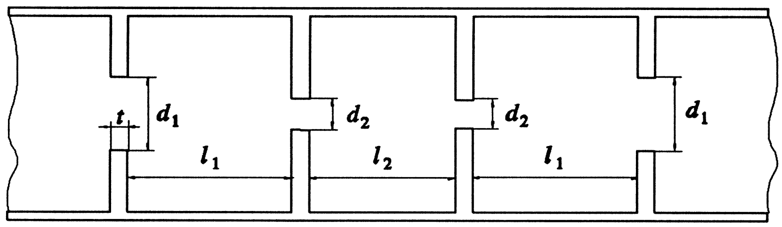

(*a*)

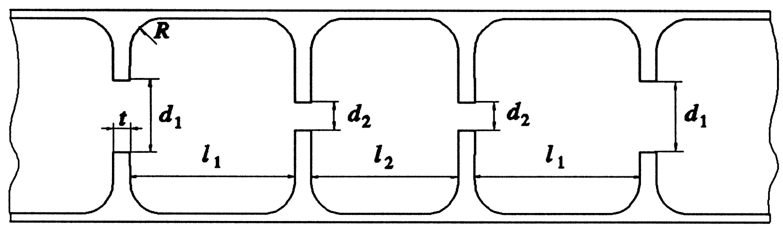

(*b*)

Fig. 2. Structures for space mapping optimization: (*a*) optimization space model, for hybrid MM/network theory; (*b*) fine model, for analysis by FEM. The waveguide cross-section is 15.8 × 7.9 mm, the thickness of the irises is t = 0.4 mm. Optimization variables are iris openings d_1, d_2 and resonator lengths l_1, l_2.

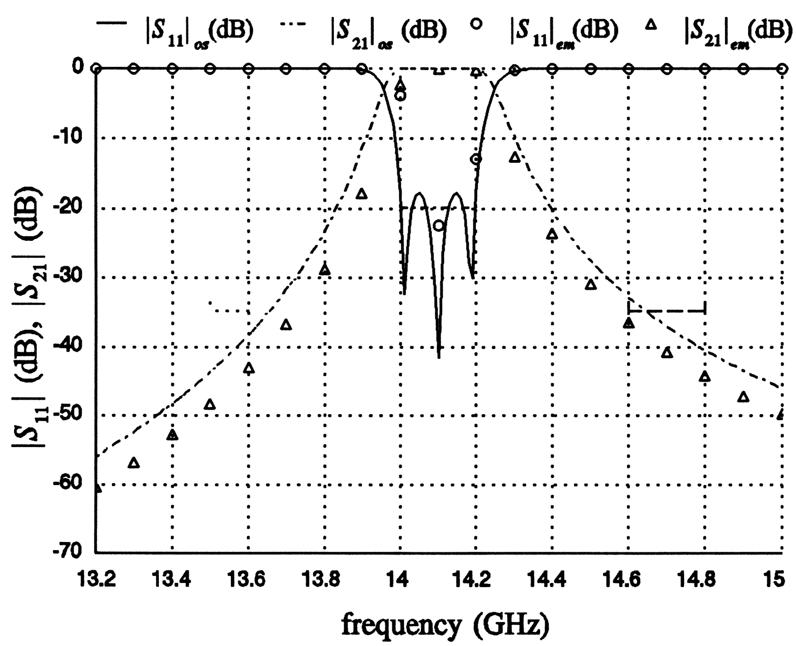

Fig. 3. Responses from both simulations of the H-plane filter based on the hybrid MM/network theory optimization solution before space mapping optimization.

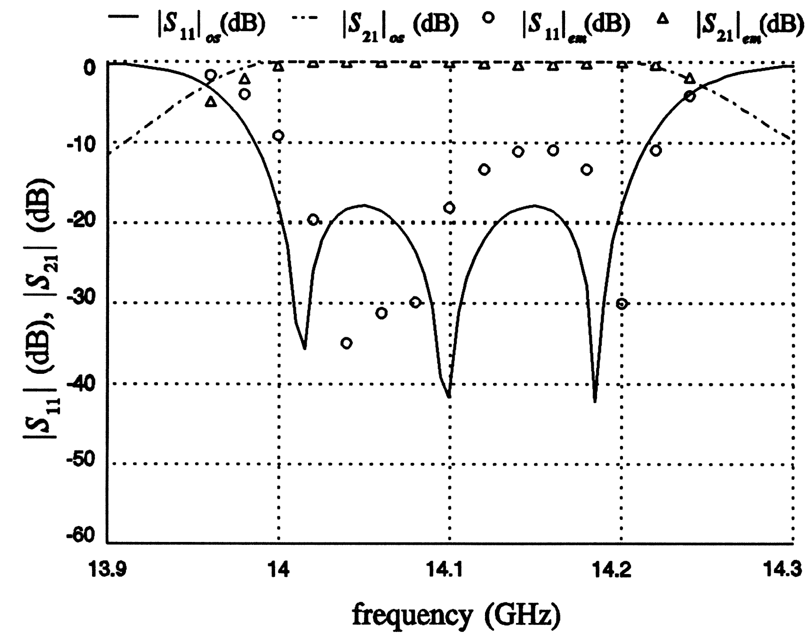

Fig. 4. Responses from both simulations of the H-plane filter before space mapping optimization, focusing on the passband.

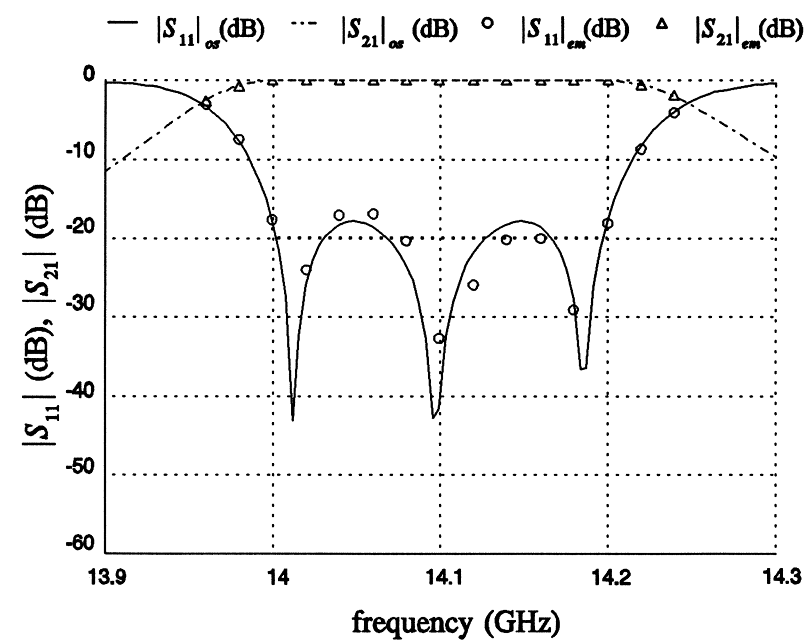

Fig. 5. Space mapping optimized FEM response of the H-plane filter compared with the optimal OS response target. Optimal results have been obtained after only 4 simulations by Maxwell Eminence.

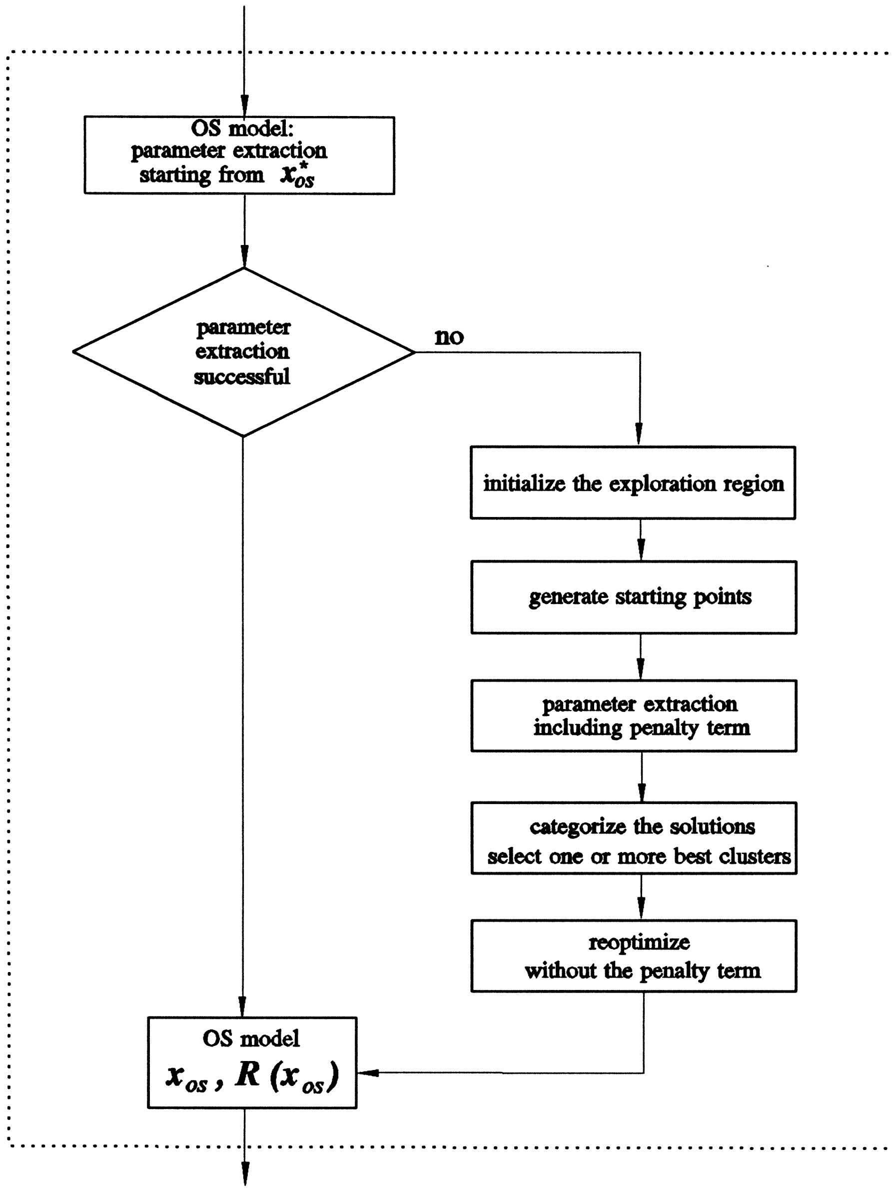

Fig. 6. Flow diagram of the statistical parameter extraction procedure.

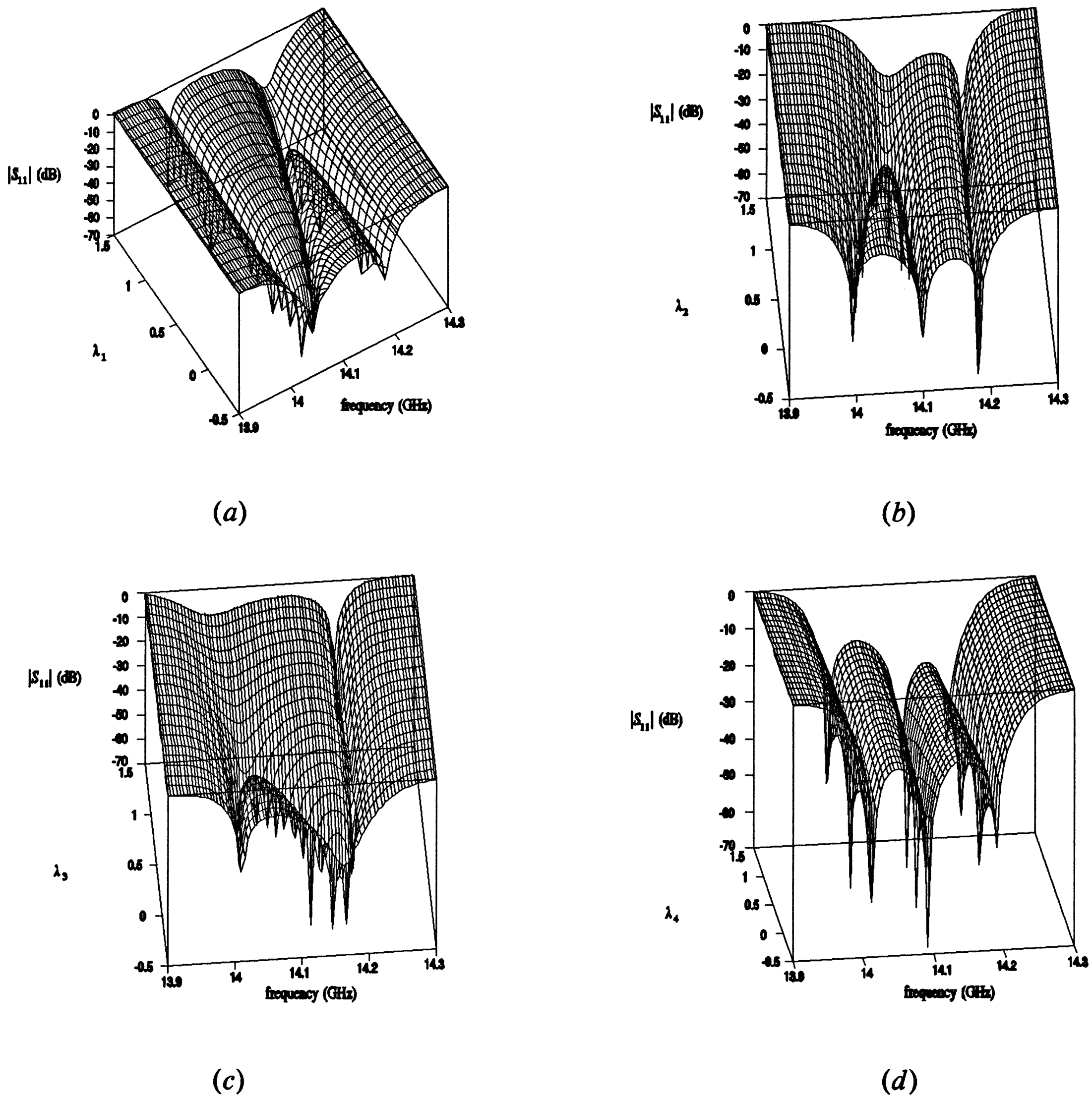

Fig. 7. Variation of responses w.r.t. each parameter, with total changes defined by the first space mapping step. $\lambda_i = 0$ at x_{os}^* and $\lambda_i = 1$ at x_{os}^1. Variation of: (*a*) opening of the first iris d_1; (*b*) opening of the second iris, d_2; (*c*) length of the first resonator; (*d*) length of the second resonator.

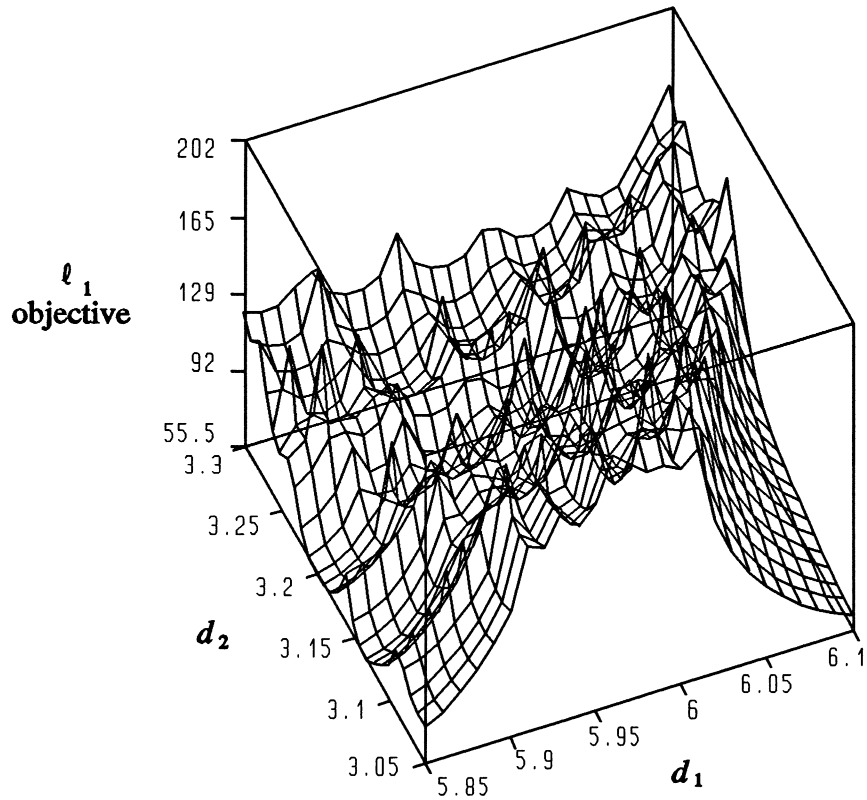

Fig. 8. Variation of ℓ_1 objective w.r.t. iris openings d_1 and d_2. Other parameters were held fixed at values corresponding to x_{os}^*.

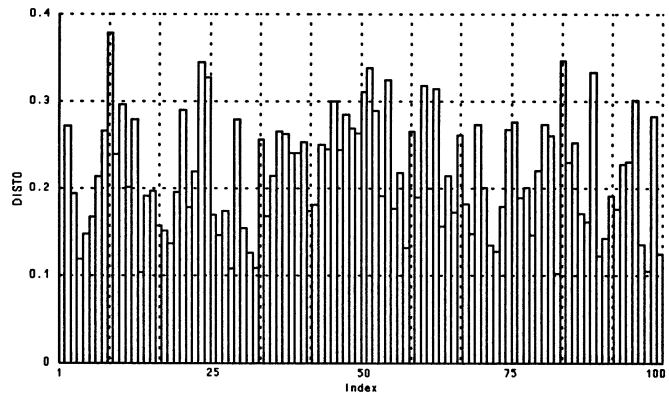

(*a*)

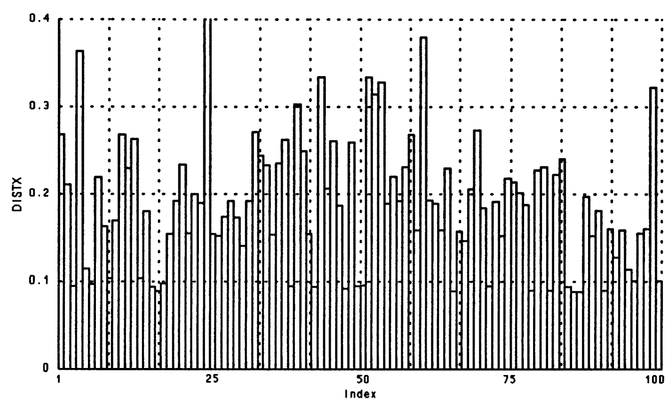

(*b*)

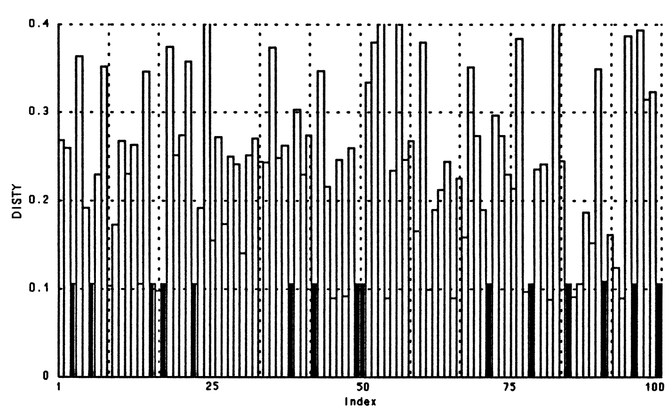

(*c*)

Fig. 9. Statistical parameter extraction: (*a*) Euclidean distances of the starting points generated randomly; (*b*) Euclidean distances of converged point after the first step; (*c*) Euclidean distances of converged point after the second stage of statistical parameter extraction. All distances are measured from the standard starting point x_{os}^*.

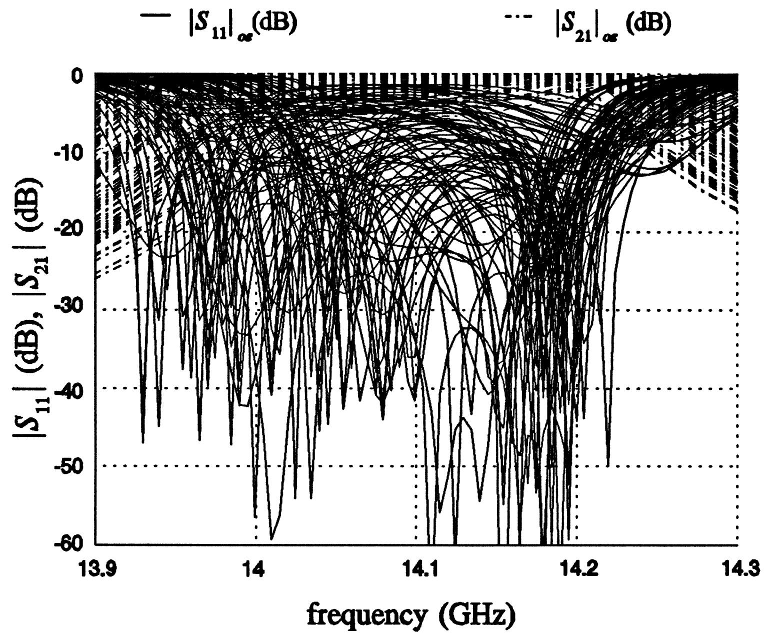

Fig. 10. Statistical parameter extraction: responses at 100 starting points generated randomly by perturbing parameters of the standard starting point.

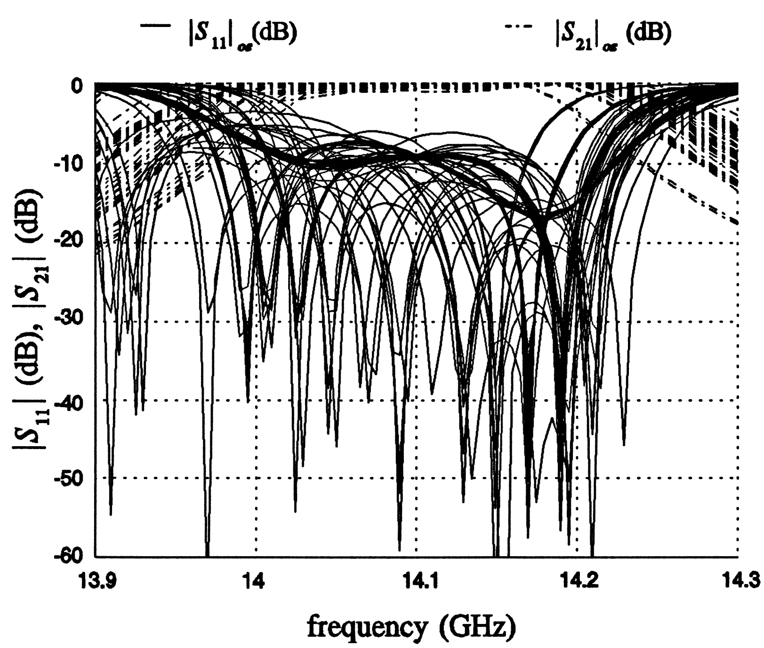

Fig. 11. Statistical parameter extraction: responses at 100 parameter extraction solution points.

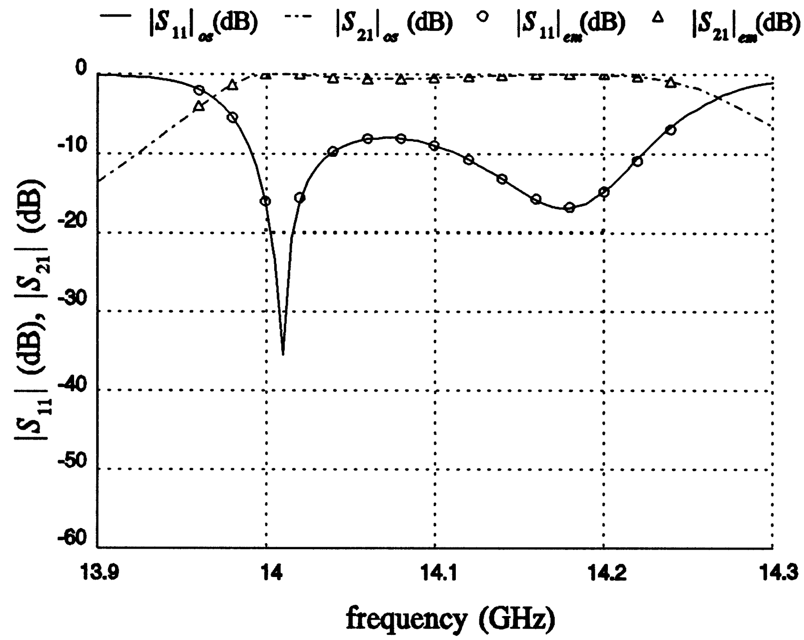

Fig. 12. MM responses corresponding to a cluster of 15 converged points obtained after statistical parameter extraction. The match to the FEM response is very good. The 15 responses are indistinguishable from each other.

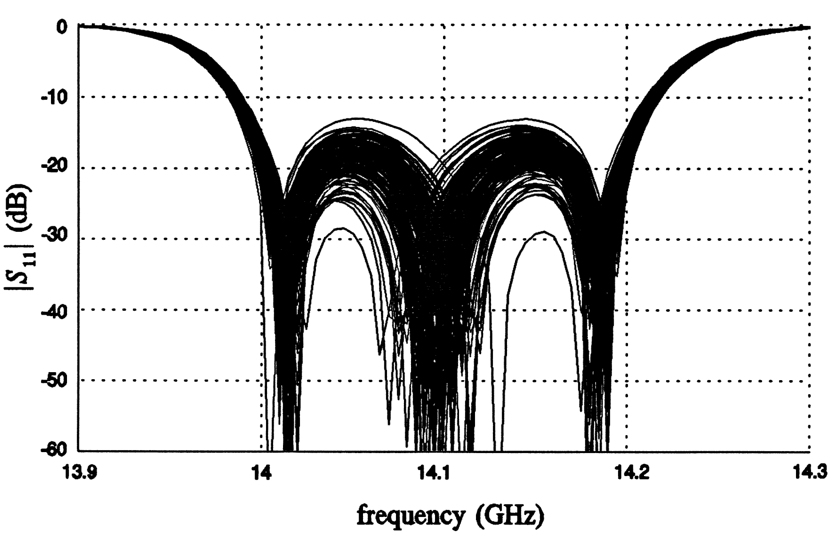

Fig. 13. Monte Carlo analysis of the H-plane filter. The parameter tolerances were statistically generated with a standard deviation of 0.0333%. The estimated yield is 88.5% out of 200 outcomes.